

PAPER • OPEN ACCESS

Functional synergy recruitment index as a reliable biomarker of motor function and recovery in chronic stroke patients

To cite this article: Nerea Irastorza-Landa *et al* 2021 *J. Neural Eng.* **18** 046061

View the [article online](#) for updates and enhancements.



PAPER

Functional synergy recruitment index as a reliable biomarker of motor function and recovery in chronic stroke patients

OPEN ACCESS

RECEIVED

3 September 2020

REVISED

14 January 2021

ACCEPTED FOR PUBLICATION

2 February 2021

PUBLISHED

18 May 2021

Original content from this work may be used under the terms of the [Creative Commons Attribution 4.0 licence](#).

Any further distribution of this work must maintain attribution to the author(s) and the title of the work, journal citation and DOI.



Nerea Irastorza-Landa^{1,2,3,4,*} , Eliana García-Cossio⁵ , Andrea Sarasola-Sanz^{1,4} , Doris Brötz¹, Niels Birbaumer^{1,6} and Ander Ramos-Murguialday^{1,4}

¹ Neuroprosthetics Group, Institute of Medical Psychology and Behavioral Neurobiology, University of Tübingen, Tübingen, Germany

² International Max Planck Research School for Cognitive and Systems Neuroscience, Tübingen, Germany

³ IKERBASQUE, Basque Foundation for Science, Bilbao, Spain

⁴ Neurotechnology Laboratory, TECNALIA, Basque Research and Technology Alliance (BRTA), Donostia-San Sebastián, Spain

⁵ neuroCare Group GmbH, Munich, Germany

⁶ Wyss Center for Bio and Neuroengineering, Geneva, Switzerland

* Author to whom any correspondence should be addressed.

E-mail: nerea.irastorza@tecnalia.com

Keywords: stroke, motor function, muscle synergies, biomarker, upper limb, neurorehabilitation

Supplementary material for this article is available [online](#)

Abstract

Objective. Stroke affects the expression of muscle synergies underlying motor control, most notably in patients with poorer motor function. The majority of studies on muscle synergies have conventionally approached this analysis by assuming alterations in the inner structures of synergies after stroke. Although different synergy-based features based on this assumption have to some extent described pathological mechanisms in post-stroke neuromuscular control, a biomarker that reliably reflects motor function and recovery is still missing. **Approach.** Based on the theory of muscle synergies, we alternatively hypothesize that functional synergy structures are physically preserved and measure the temporal correlation between the recruitment profiles of healthy modules by paretic and healthy muscles, a feature hereafter reported as the FSRI. We measured clinical scores and extracted the muscle synergies of both ULs of 18 chronic stroke survivors from the electromyographic activity of 8 muscles during bilateral movements before and after 4 weeks of non-invasive BMI controlled robot therapy and physiotherapy. We computed the FSRI as well as features quantifying inter-limb structural differences and evaluated the correlation of these synergy-based measures with clinical scores. **Main results.** Correlation analysis revealed weak relationships between conventional features describing inter-limb synergy structural differences and motor function. In contrast, FSRI values during specific or combined movement data significantly correlated with UL motor function and recovery scores. Additionally, we observed that BMI-based training with contingent positive proprioceptive feedback led to improved FSRI values during the specific trained finger extension movement. **Significance.** We demonstrated that FSRI can be used as a reliable physiological biomarker of motor function and recovery in stroke, which can be targeted via BMI-based proprioceptive therapies and adjuvant physiotherapy to boost effective rehabilitation.

Abbreviations and acronyms

FSRI functional synergy recruitment index
BMI brain-machine interface
UL upper limb

EMG electromyography
FMA Fugl-Meyer assessment
MAS modified Ashworth scale
VAF variance accounted for
nCC normalized correlation coefficient

1. Introduction

Recent evidence suggests that complex neuromuscular coordination may be achieved through a combined activation of a limited number of motor primitives in different vertebrate animal models [1–4] and humans [5–7], which are hypothesized to be encoded in neuronal networks at brainstem and spinal levels rather than in the cortex [1, 8, 9]. These primitives, commonly referred to as muscle synergies, are described as individual control modules defined as constant weight coefficients related to an ensemble of muscles. When synchronously recruited by cortical descending neural commands (described as synergy activation patterns [5, 10, 11]), these individual neural modules co-activate in turn the motoneurons of a group of muscles with specific weight coefficients, simplifying motor control [5, 10, 12–17].

In stroke survivors, disruptions in the descending motor control signals arise as a consequence of the cerebrovascular accident, leading to abnormal recruitment of muscle synergies [1, 8, 9]. Consequently, inappropriate muscle coordination [5] results in poor motor performance of the affected UL [17–19]. Due to their potential to convey information on the neurophysiology of the altered nervous system and subsequent motor impairment, different muscle synergy features have been proposed as quantitative biomarkers for UL motor function in stroke [20–25].

Most studies have approached muscle synergy analysis by investigating differences in synergy structure expression between healthy and paretic ULs in stroke patients. Chronic patients with diverse brain lesions have shown a high level of preservation (i.e. degree of similarity between paretic and healthy synergy structures), despite the presence of abnormal EMG patterns and moderate impairment [5]. In contrast, severely impaired patients with heterogeneous chronicity and lesions presented a significantly lower degree of preservation [22, 23, 26]. Likewise, the level synergy structure preservation has been found to be related to the degree of motor function in patients with mild-to-moderate impairment [27] and occasionally to directly correlate with arm motor function scores [22]. Additionally, certain non-preserved synergy structures in severely affected ULs could be explained as a merging or fractionation of healthy structures [23], mechanisms that have been found to correlate with UL motor impairment level and chronicity, respectively. Moreover, some longitudinal studies have reported non-significant changes in the degree of synergy structure preservation in severely impaired subacute [28] and moderately impaired chronic [29] patients after significant motor improvement, while others have described slight structural changes [30], in some cases toward a healthy structure pattern [31, 32].

Based on muscle synergy theory, it could be hypothesized that stroke does not necessarily affect the inner structure of synergies but their temporal recruitment by altered descending supraspinal signals, thus compromising contralateral motor performance [5, 28, 33, 34]. Some authors argue that merging and fractionation could be indeed explained by the inability of patients to independently and simultaneously activate physically preserved normal synergy structures, respectively, rather than by alterations of their intrinsic structure [8]. In fact, previous findings in lower limb muscle synergies have confirmed a high similarity of paretic synergy modules in comparison to healthy subjects whereas changes in their temporal recruitment patterns directly correlated with motor impairment [35]. Various groups have also reported altered synergy activation patterns in the paretic UL with respect to the healthy activation coefficients in mild-to-moderately impaired subacute [28, 36] and chronic patients [5]. Moreover, various groups have documented slight modifications in the correlation between paretic and healthy synergy temporal activations after rehabilitation [28, 29], indicating a certain degree of adaptability in the flow of descending cortical commands. However, it is unclear if the reshaping of recruitment patterns shifted towards the direction of healthy coefficients or maladaptive patterns [28, 29]. These previous studies have conventionally compared temporal recruitment profiles of homologous but slightly different pathological and functional synergy structures expressed in the paretic and healthy muscle activity, respectively. Thus, these approaches inevitably entail inter-limb variability in temporal activations of synergies due to the assumed differences in their structures rather than to the possibly different cortical strategies for their recruitment, which could potentially reflect the degree of motor function of the affected limb.

In our work, based on previous evidence and muscle synergy theory, we hypothesize that functional synergy modules, although not explicitly expressed in the paretic EMG, are physically preserved in stroke patients. Thereby, in contrast to conventional synergy analyses assuming inter-limb differences in synergy structure, we propose a feature to measure the ability to elicit correct temporal recruitment patterns of a common set of functional synergies during paretic limb motor control in comparison to the healthy one. Thus, we investigated this and other conventional muscle synergy features before and after intensive BMI-based motor rehabilitation combined with physiotherapy in a group of severely unilaterally impaired chronic stroke patients and explored the correlations between these features and motor function as well as recovery. Finally, we explore the relevance of the BMI contingency to modify task-specific synergy recruitment.

2. Methods

2.1. Patients

A total of 36 severely impaired chronic stroke patients were initially considered in this study. All patients fulfilled the following inclusion criteria: (a) no residual finger extension in the paretic hand (modified FMA score for hand and fingers at admission: 3.69 ± 3.03 , range: 0–11); (b) time since stroke at least 10 months; (c) age between 18 and 80 years; (d) no psychiatric or neurological condition other than stroke; (e) no cerebellar lesion or bilateral motor deficit; and (f) ability to understand and follow instructions (mini-mental state score above 21). Further inclusion criteria were described in [37]. After a patient selection procedure based on the quality of EMG recordings (see figure S1 in supplementary material and section 2.5 (available online at stacks.iop.org/JNE/18/046061/mmedia)), a final pool of 18 patients (12 males, mean age 54.66 ± 12.01 years, mean time after stroke 82.11 ± 65.20 months) were included in this analysis. Ten patients had a subcortical lesion and eight had a mixed (subcortical and cortical) lesion. A cortical lesion was considered to be localized exclusively at the sensorimotor cortex. The assessment of lesion extension was carried out by an experienced radiologist based on the patients' T1 MR images (table 1). The study was approved by the ethics committee of the Faculty of Medicine of the University of Tübingen and all the patients gave informed consent before entry.

2.2. Rehabilitative intervention

Patients underwent a neurorehabilitative intervention that consisted in a daily BMI training (1 h) followed by behavioral physiotherapy (1 h) during a total mean period of 17 ± 1.8 d. All patients received hand-BMI therapy by controlling a hand orthosis that performed the extension/flexion of the fingers. Some patients additionally received arm-BMI training using an arm orthosis attached to their paretic upper- and fore-arm that enabled the extension/flexion of the arm and the elbow (0–11 sessions, mean: 5.11 ± 4.27 sessions) depending on their initial arm function score (i.e. individuals with a lower aFMA score received more sessions of arm orthosis BMI control). All patients were instructed to voluntarily attempt to move their paralyzed hand or arm, thus causing the desynchronization of sensorimotor rhythms (SMR) in the ipsilesional motor cortex that were measured with electroencephalography. During BMI operation, the experimental group received a contingent positive (C+, $n = 10$, orthosis movement feedback concurrent with their movement intention) feedback, whereas the control group ($n = 8$) received either a random (R, $n = 5$, i.e. orthosis movement was not associated with the patient's SMR oscillations) or contingent negative (C-, $n = 3$, i.e. orthosis movement was opposite to the decoded movement intention) feedback.

Further details of the intervention are described in [37]. Demographics, lesion location and intervention group are summarized in table 1.

2.3. Clinical assessment

The level of motor impairment of the affected UL of each patient was evaluated before and after the intervention using the modified version of the FMA for the hand/fingers (hFMA, 0–24), for the upper-arm (aFMA, 0–30) and their combination (cFMA, 0–54), excluding items related to upper extremity sensation, pain, coordination, speed and reflexes [37, 38]. The MAS was used for measuring spasticity (0–56). The level of motor function of the affected UL of each patient was assessed two months before the rehabilitative intervention (pre1), one day before the first session (pre2) and immediately after intervention (post measurement). For comparative purposes of the collected clinical scales before and after intervention, pre1 and pre2 measurements were averaged and considered as a baseline score (pre) to reduce variability between measurements that was not ascribed to the effect of the intervention [37, 39, 40].

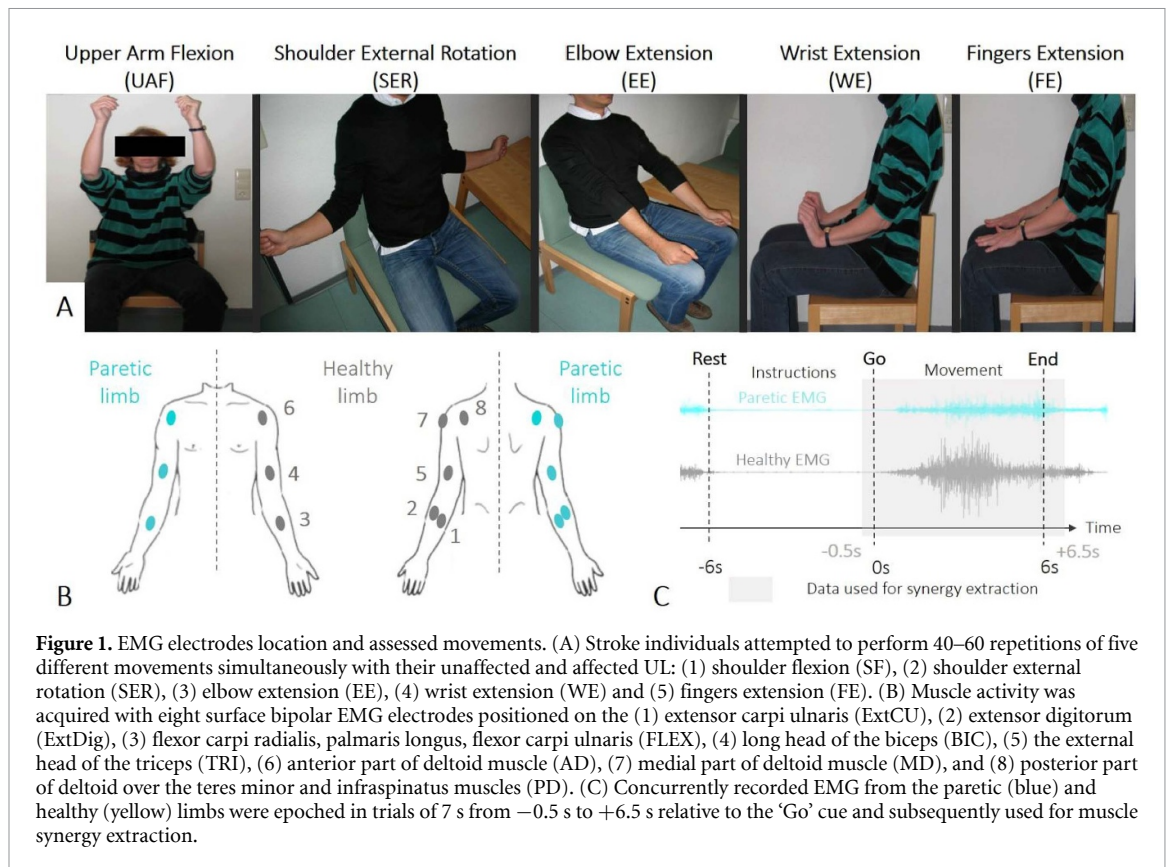
2.4. EMG recordings and motor tasks

EMG activity of each patient was also measured before (pre) and after (post) the rehabilitative intervention. Surface EMG activity of the paralyzed and healthy ULs were recorded using Ag/AgCl electrodes placed on the following muscles in both limbs: (a) extensor carpi ulnaris (ExtCU), (b) extensor digitorum (ExtDig), (c) flexor carpi radialis, palmaris longus, flexor carpi ulnaris (FLEX), (d) biceps (BIC), (e) triceps (TRI), (f) anterior (AD), (g) medial (MD), and (h) posterior part of deltoid and infraspinatus (PD). The ground electrode was placed over the affected side clavicle (figure 1(B)). EMG signals were acquired with a BrainAmp amplifier from Brain Products GmbH (Munich, Germany) at 2500 Hz.

Patients performed on average 40–60 trials of five different bilateral movements simultaneously with both ULs (paretic and healthy): starting from a relaxed position with both hands resting on their lap, (a) shoulder flexion (SF), (b) shoulder external rotation (SER), (c) elbow extension (EE), (d) wrist extension (WE) and (e) finger extension (FE) (figure 1(A)). These motor tasks were selected specifically because of their analogy to the items used to evaluate the affected extremity function in the FMA scale. After an instruction period of 6 s in rest posture, a 'Go' cue was presented and a movement period of 6 s was given to attempt to reach and maintain the instructed final posture by eliciting isometric co-contraction of muscles. Compensatory movements were discouraged. The end of the movement period was indicated by a second cue 'End' and immediately after an inter-trial period between 4 and 7 s was given to return to the initial resting position (figure 1(C)).

Table 1. Patient demographic information and description of lesion location.

ID	BMI Feed-back group	Sex	Age	Months since stroke	Lesion	Lesion location
1	Exp	M	29	25	Mix	Frontal and parietal lobe. Inferior frontal gyrus; precentral gyrus. Insula cortex, external capsule, CI, head of caudate nucleus, genu, putamen, thalamus.
2	Exp	M	65	45	Sub	Parietal lobe. White matter of inferior frontal gyrus; pre and postcentral gyrus; supramarginal gyrus. Corona radiata, thalamus, genu, partially CI, external capsule. Also affection of the white matter underlying the right insular cortex.
3	Exp	M	60	130	Sub	Parietal lobe. White matter of Precentral gyrus. Corona radiata, anterior CI, putamen, external capsule, thalamus, insula.
4	Exp	M	57	122	Sub	Corona radiata, external capsule, putamen, posterior CI, thalamus.
5	Exp	M	47	80	Sub	CI, genu, external capsule, claustrum, putamen, head of caudate nucleus, thalamus.
6	Exp	F	72	44	Sub	Frontal and parietal lobe. White matter of inferior frontal gyrus; pre and postcentral gyrus; supramarginal gyrus. Multiple necrotic vesicles. Trunk of corpus callosum, head of caudate nucleus, corona radiata, putamen, external capsule, CI, genu, thalamus.
7	Exp	M	69	72	Sub	Frontal and parietal lobe. Extensive white matter hypodensity of inferior frontal gyrus and precentral gyrus. Corona radiata, head of caudate nucleus, CI, genu, external capsule, putamen, thalamus, insula.
8	Exp	F	55	45	Sub	Corona radiata, head of caudate nucleus, external capsule, CI, genu, putamen, thalamus, globus pallidus, claustrum.
9	Exp	M	48	45	Sub	CI, genu, external capsule, putamen, thalamus, claustrum, head and tail of caudate nucleus, corona radiata, insula.
10	Exp	F	53	30	Sub	Corona radiata, external capsule, thalamus, putamen, CI, genu.
11	Control	F	66	23	Mix	Frontal and parietal lobe. Superior, medial, middle and inferior frontal gyrus; pre and postcentral gyrus. Frontal, parietal and temporal lobe. Middle and inferior frontal gyrus; pre and postcentral gyrus; supramarginal gyrus; middle and inferior temporal gyrus. Corona radiata, head of caudate nucleus, CI, genu, external capsule, claustrum, putamen, trunk of corpus callosum, insula, thalamus.
12	Control	M	69	89	Mix	Frontal and parietal lobe. Precentral gyrus. Corona radiata, thalamus, putamen, posterior CI, claustrum, external capsule, insula.
13	Control	M	47	232	Mix	Frontal and parietal lobe and the adjacent white matter. Superior, medial, middle and inferior frontal gyrus; pre and postcentral gyrus; supramarginal gyrus. Corona radiata, head of caudate nucleus.
14	Control	M	54	121	Mix	Corona radiata, CI, genu, thalamus, external capsule, putamen, claustrum, insula and adjacent white matter.
15	Control	M	50	215	Sub	Parietal and occipital lobe and the adjacent white matter, multiple necrotic vesicles in the parietal lobe underneath the post-central and pre-central gyrus, gray matter of the post- and precentral gyrus partly intact
16	Control	M	59	14	Mix	Cortical stroke affecting the frontal- and parietal lobe (pre- and postcentral gyrus). Corona radiata, capsula externa affected. Hypodense white matter of the frontal and parietal lobe.
17	Control	F	30	15	Mix	Frontal and parietal lobe. Pre-postcentral gyrus.
18	Control	F	54	131	Mix	Frontal and parietal lobe. Inferior frontal gyrus; precentral gyrus. Insula cortex, external capsule, CI, head of caudate nucleus, genu, putamen, thalamus.



2.5. EMG pre-processing and rejection of artefacted data

EMG signals were band-pass filtered (4th order Butterworth filter, 20–450 Hz) and notch filtered (50 Hz and harmonics). The envelope of the rectified EMG signals was calculated using a low-pass filter of 1 Hz (2nd order Butterworth filter) and re-sampled to ten samples per second. The activity of all electrodes from the same limb (healthy or parietic) were normalized to the mean variance of all EMG channels activity of that same limb in order to correct for inter-arm and inter-session EMG amplitude differences due to changes in electrode impedance, while keeping the inter-muscular relative amplitude. EMG data were epoched in trials of 7 s (from -0.5 s to $+6.5$ s relative to the ‘Go’ cue), thus including a 0.5 s rest interval before the initiation of the movement and 0.5 s after the instruction cue to return from the final movement position to rest (figure 1(C)). Each trial and EMG channel were baseline-corrected by subtracting the average activity during the inter-trial interval in rest position that preceded each following activity window. All trials in each EMG electrode were visually examined for each patient and measurement for artifacts detection. Patients that presented at least one electrode with more than 50% artefacted trials or constant bad impedance during the entire measurement were discarded from the subsequent analysis with the objective of maintaining data dimensionality across subjects for comparative purposes. For each remaining patient, we created

two datasets (pre and post intervention) comprising EMG activity from identical number of muscles [8] and identical number of trials of each type of movement for each UL (defined by the minimum number of artifact-free trials for each movement between limbs).

2.6. Muscle synergies extraction and optimal number of synergies

After EMG pre-processing and subsequent artefacted data rejection, muscle synergies were extracted from the pre-processed and concatenated EMG data including trials of the performed five movements by applying a non-negative matrix factorization (NNMF) algorithm [41, 42]. NNMF consists in the factorization of multi-muscle EMG signals into two matrices that represent those time-invariant weighted activations of a group of muscles (W , synergy structures) and time-variant activation profiles (C , synergy recruitment patterns) [17, 26, 43, 44]. Thus, the factorization of EMG signals into these two matrices aims at representing the individual control modules encoded in neuronal networks at brainstem and spinal levels [1, 8, 9] and the neural drive for the control of such modules, respectively [45, 46]. The factorization of muscle activity is represented by the following equation:

$$m(t) = \sum_{i=1}^n C_i(t) \cdot W_i$$

where $m(t)$ represents the EMG activity vector ($m \times t$ matrix; m = number of muscles, t = time points), $C_i(t)$ are the time-varying activation patterns of each synergy i in each time point t ($n \times t$ matrix; n = number of synergies, t = time points) and W_i denote fixed weighting vectors whose elements represent the relative contribution of the muscles to each synergy i ($m \times n$ matrix; m = number of muscles, n = number of synergies). An example of this matrix factorization is represented in figure 2(A).

In order to determine the optimal number of synergies for each dataset, this factorization procedure was performed increasing the number of synergies from 1 to 8 (number of recorded muscles in each limb) and repeated in a 20-fold cross-validation procedure [26, 47]. This procedure was performed for real and shuffled EMG data that was generated by randomizing the order of the EMG data points across muscles and time. The VAF [17, 36, 48] was calculated for each muscle and the minimum number of synergies that enabled an EMG reconstruction with a global VAF (mean VAF of all eight muscles) above 95% [2, 27, 49] and that adding another synergy did not increase global VAF > 3% [17] was initially selected as the optimal number of synergies for each patient, session and limb. In order to avoid variances due to the dimensionality of the reference set of healthy synergies and enable an inter-session comparison, we opted for setting the same number of healthy modules for all patients [17, 27, 28, 49] and sessions. We defined this number based on the most frequent optimal number of synergies among all patients and both assessment sessions together. In contrast, the optimal number found in the paretic limb was maintained unequal for each subject in order to capture possible reduced synergy dimensionality and merging or fractionation mechanisms in each individual [23] (further details on methods for muscle synergy extraction, VAF and selection of optimal number of synergies in supplementary methods). Therefore, the synergy structures of the healthy and paretic limbs used for subsequent analyses (cluster analysis, preservation, merging and fractionation indexes, and FSRI) were extracted based on the number of synergies selected for each limb according to the aforementioned conditions.

2.7. Cluster analysis on muscle synergies

Cluster analysis was applied as a descriptive approach to visualize the general modular organization, as well as possible overall modifications over time in the affected and non-affected limbs. Synergy structures (vectors including the weightings of eight muscles) extracted from every patient before and after the intervention in each limb (healthy and paretic) were pooled together in four independent datasets (healthy modules in PRE and post, paretic modules in PRE and POST) and were clustered for a general comparison of muscle modules in each limb between assessment

sessions. Optimal synergies extracted from each UL of all patients before and after the intervention were normalized to the Euclidean norm, separately pooled and clustered for characterizing the stability and general modifications in synergy weightings in the non-affected and affected limbs, respectively. An independent hierarchical cluster analysis was applied for each limb's dataset using statistic-toolbox functions in Matlab. The similarity indices between the muscle weights of every pair of synergies were calculated using *pdist* function (Minkowski distance option, $p = 2$, equivalent to Euclidean distance), which were subsequently considered to group their related synergies into a binary, hierarchical cluster tree by applying the *linkage* function (Ward option) and finally the optimal extension and objects distribution of such tree was determined by the *cluster* function [26, 44, 50]. The optimal amount of clusters was determined based on the silhouette index [26], where values close to one reflect a low intra-cluster variance and a high inter-cluster difference, and thus a more optimal clustering. The number of clusters from 2 to 16 with the highest silhouette index and with clusters including at least two synergy structures was selected as the optimal number of groups of synergies that most adequately represented the general synergy expressions across all patients. The degree of similarity of synergy cluster mean weightings obtained before and after therapy was measured by computing the scalar product and clusters showing highest similarity were paired and considered as homologous synergy clusters.

2.8. Preservation, merging and fractionation indexes

We first studied the three principal features widely adopted in the literature investigating inter-limb (healthy and paretic) structural differences in muscle synergies. Preservation index was computed by averaging the scalar product between paired synergy structures of the healthy and paretic limbs after normalization of weighting vectors to the Euclidean norm [6, 47]. Each synergy in the paretic limb was matched to any of the still un-paired synergies of the healthy that presented the highest degree of similarity when compared to it (i.e. highest scalar product, with a maximal value of 1). This procedure was performed in a one-to-one basis, limiting the matching of each paretic synergy to a single healthy one and occasionally leaving additional unpaired healthy modules (superior in number) not considered for inter-limb synergy comparison. Preservation index indicates the degree of similarity of synergy structures found in the paretic limb with respect to the healthy one.

Merging and fractionation patterns were computed as described in [23], considering them as separate processes from preservation (i.e. all extracted synergy structures were included for merging and preservation analysis). Briefly, merged

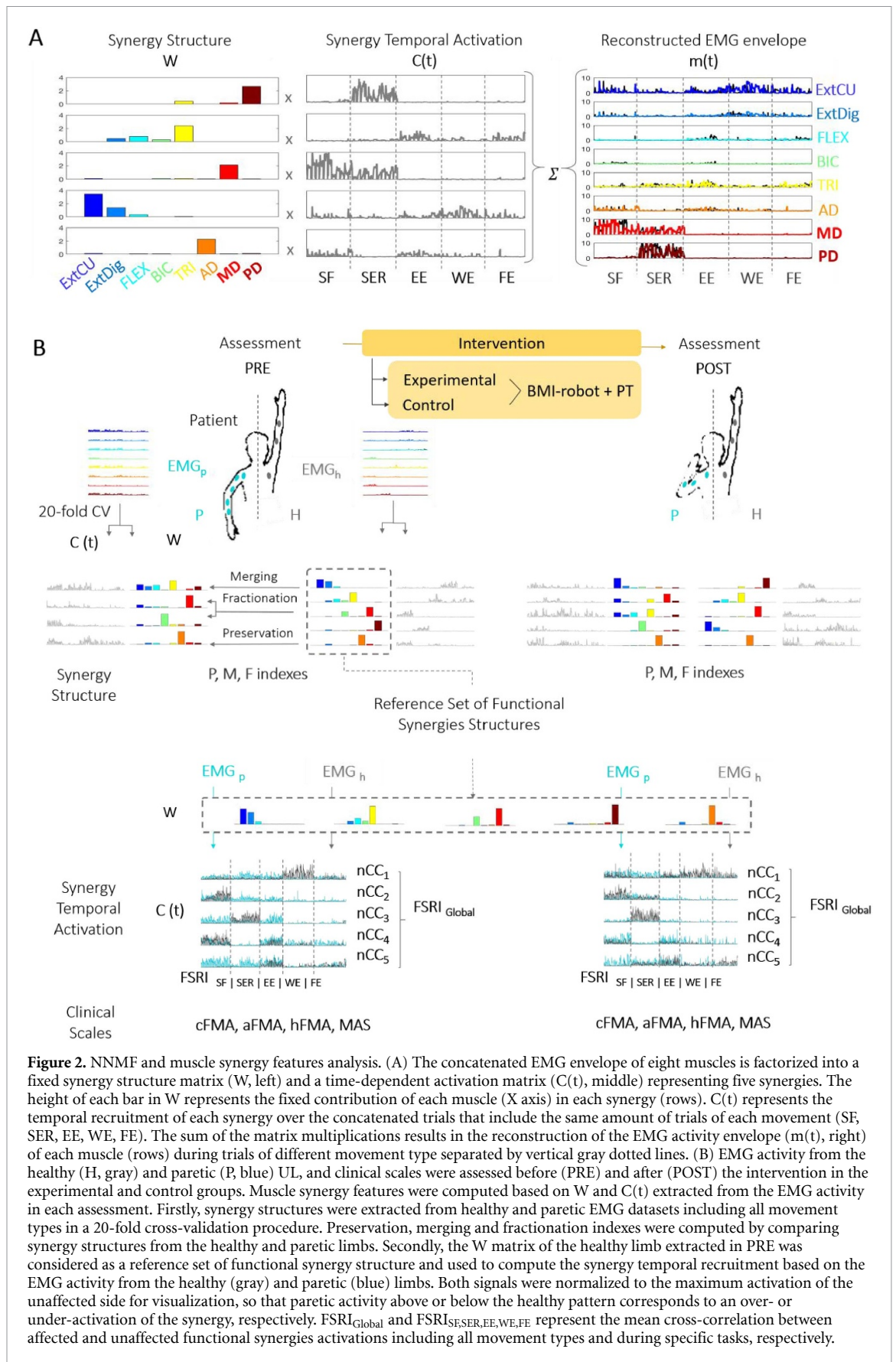


Figure 2. NNMF and muscle synergy features analysis. (A) The concatenated EMG envelope of eight muscles is factorized into a fixed synergy structure matrix (W , left) and a time-dependent activation matrix ($C(t)$, middle) representing five synergies. The height of each bar in W represents the fixed contribution of each muscle (X axis) in each synergy (rows). $C(t)$ represents the temporal recruitment of each synergy over the concatenated trials that include the same amount of trials of each movement (SF, SER, EE, WE, FE). The sum of the matrix multiplications results in the reconstruction of the EMG activity envelope ($m(t)$, right) of each muscle (rows) during trials of different movement type separated by vertical gray dotted lines. (B) EMG activity from the healthy (H, gray) and paretic (P, blue) UL, and clinical scales were assessed before (PRE) and after (POST) the intervention in the experimental and control groups. Muscle synergy features were computed based on W and $C(t)$ extracted from the EMG activity in each assessment. Firstly, synergy structures were extracted from healthy and paretic EMG datasets including all movement types in a 20-fold cross-validation procedure. Preservation, merging and fractionation indexes were computed by comparing synergy structures from the healthy and paretic limbs. Secondly, the W matrix of the healthy limb extracted in PRE was considered as a reference set of functional synergy structure and used to compute the synergy temporal recruitment based on the EMG activity from the healthy (gray) and paretic (blue) limbs. Both signals were normalized to the maximum activation of the unaffected side for visualization, so that paretic activity above or below the healthy pattern corresponds to an over- or under-activation of the synergy, respectively. $FSRI_{Global}$ and $FSRI_{SF,SER,EE,WE,FE}$ represent the mean cross-correlation between affected and unaffected functional synergies activations including all movement types and during specific tasks, respectively.

synergies in the paretic limb were considered as linear combinations of unaffected synergies, while fractionation was described as the linear combination of affected synergies that could fairly reconstruct a healthy synergy. For merging and fractionation index calculation, the contribution of each paretic module was limited to either one or several merged modules, or to a single fraction of a healthy synergy, determined by the mechanism that led to a higher synergy reconstruction (for further details on model computation and constraints see [23]). In both cases, affected modules were considered as combinations (merging) or fractions of healthy synergies if the similarity between the compared merged/fractionated paretic and healthy synergies was >0.75 [26]. The merging or fractionation indexes were considered 0 if the mechanism was not present in the studied synergies. Thus, merging index was represented by the ratio between number of paretic modules that could be reliably represented as combinations of healthy synergies and the total number of paretic modules, whereas fractionation index was defined as the ratio between the number of affected synergies that were considered as fractions of healthy modules and the total number of paretic modules.

2.9. FSRI

We considered the synergy structures extracted from the healthy limb before treatment in each subject as the patient-specific reference set of functional synergies (FSRI computation approach is represented in figure 2(B)) whose structures have not been influenced by any familiarization/adaptation process to the evaluated motor task [51]. These synergies represent the potential motor units that the ipsilesional sensorimotor cortex should aim at recruiting in order to produce normal motor performance. After defining the set of functional synergies of each patient in PRE, the temporal activation patterns of such synergy structures were calculated independently from the simultaneously recorded healthy and paretic EMG recordings during bilateral movements. Finally, the normalized cross-correlation coefficient (nCC, range: [0,1]) at lag 0 (i.e. assuming simultaneous bilateral movements) was computed between temporal activations ($C(t)$) [27] derived from each of synergy structure (W) of the reference set of functional synergies. We calculated these correlations between the sequentially concatenated trials of temporal synergy recruitment profiles for all movement conditions together and individually for each individual movement type (SF, SER, EE, WE, FE). We denominated the mean of these five nCC coefficients (from the set of five healthy synergy structures) as the FSRI, resulting in $FSRI_{Global}$ and task-specific FSRI values ($FSRI_{SF,SER,EE,WE,FE}$ for individual movements). We considered this feature as the degree of temporal similarity of the activation profiles of healthy functional control modules manifested in the paretic muscles in reference to a healthy

homologous pattern. This feature was calculated separately for the PRE and POST assessment sessions.

2.10. Statistical analysis

Normality of variables and homogeneity of variances of the data were first assessed by applying a Shapiro–Wilk and a Levene’s test, respectively, to determine if the required assumptions to carry out parametric tests were met. If violation of any of these conditions occurred, data were either log-transformed ($\log(x + 1)$, in order to handle zero values) to meet parametric conditions or non-parametric tests were alternatively applied.

General pre-post changes in clinical scores and synergy features were analyzed by applying paired t-test and Wilcoxon signed-rank test for normally and non-normally distributed data, respectively. Correlations between (a) pre-therapy and (b) pre-post differences in synergy features and (a) pre-therapy and (b) pre-post changes in clinical (ordinal) scores and chronicity were computed with Spearman’s rank correlation coefficient. All patients ($n = 18$) were included for this test and statistical significance was set at p -value <0.05 for all tests.

Additionally, pre-post intervention changes in clinical scales and synergy features were compared in the experimental and control groups to study the effect of the BMI feedback contingency. For variables fulfilling normality and homogeneity of variance, a mixed ANOVA with one within-subjects factor (TIME: pre, post) and one between-subjects factor (GROUP: C, NC) was performed. For non-Gaussian variables, we compared the pre-post difference in the analyzed scores between intervention groups by applying a two-tailed unpaired test (normal distribution) or a non-parametric Mann–Whitney U test.

3. Results

3.1. Clinical improvement

Although not all patients improved motor function after therapy, the analysis of pre-post changes in clinical scales of the entire group of patients ($n = 18$) revealed a general significant improvement in cFMA ($p = 0.012$) and aFMA ($p = 0.026$) (figure S2). Moreover, the intervention led to a non-significant increase in hFMA ($p = 0.054$) (figure S2). Patients did not present a significant reduction in the level of spasticity (MAS, $p = 0.29$) after the intervention. Pre and post-therapy clinical scores of individual patients are reported in table 2.

3.2. Number of optimal synergies

Original EMG activity presented a modular organization evidenced by the abruptly increase in the global VAF (blue lines in figure S3(A)), while the shuffled (structureless) data increased linearly (gray lines in figure S3(A)). Modular activity of the healthy UL could be typically represented using four (five

Table 2. Clinical scores before and after neuro-rehabilitative intervention.

Patient	cFMA		aFMA		hFMA		MAS	
	PRE	POST	PRE	POST	PRE	POST	PRE	POST
P1	15	18	13.50	15	1.50	3	5.50	11
P2	3.50	5	1.50	3	2	2	8.50	8
P3	9.50	12	6	10	3.50	2	21.50	16
P4	17	20	12	15	5	5	19.50	21
P5	12	16	9.50	13	2.50	3	3.50	1
P6	2	3	1.50	3	0.50	0	5.50	0
P7	5.50	9	5	7	0.50	2	13	14
P8	16.50	24	9	16	7.50	8	3	2
P9	7.50	14	3.50	9	4	5	3.50	5
P10	5	5	5	4	0	1	27.50	25
P11	16.50	21	14.50	17	2	4	6	6
P12	26	22	24	19	2	3	2	2
P13	13.50	10	10.50	8	3	2	8.50	10
P14	16	26	10.50	15	5.50	11	4.50	3
P15	33.50	34	22.50	23	11	11	8.50	3
P16	18	16	15	13	3	3	2.50	2
P17	33.50	37	24	26	9.50	11	7.50	6
P18	8.50	10	5	7	3.50	3	12.50	14
Total mean ± std	14.39 ± 9.23	16.78 ± 9.55	10.69 ± 7.20	12.39 ± 6.59	3.69 ± 3.03	4.39 ± 3.50	9.06 ± 7.20	8.28 ± 7.25
<i>p</i> -value	<i>p</i> = 0.012		<i>p</i> = 0.026		<i>p</i> = 0.054		<i>p</i> = 0.29	

aFMA: arm FMA; hFMA: hand FMA; cFMA: combined arm and hand FMA; std: standard deviation. Statistically significant pre-post differences are highlighted by *p*-values in bold.

patients in PRE, nine patients in POST) or five synergies (nine patients in PRE, six patients in POST), with only three and two patients needing less modules in pre and post sessions, respectively (see figure S3(B)). Although a single subject required at least six synergies in both assessment sessions to strictly fulfill predefined conditions, five synergies already enabled a mean global VAF very close to the adopted threshold (94.88% in pre and 94.22% in post). In view of these results and with the objective of simplifying healthy vs. paretic synergy comparisons across patients, the optimal number of healthy modules was set to five for all subjects, as previously adopted by other authors [17, 27, 28, 49]. The optimal number of synergies of the paretic limb was set to the number of modules that fulfilled the predefined criteria in order to capture the adopted modular control in the paretic limb of each patient and compare possible modifications due to the intervention.

3.3. Cluster analysis

Cluster analysis revealed that eight and seven groups of muscle synergies could optimally represent the general modular organization of the healthy (figure 3(A)) and paretic (figure 3(B)) muscle activations in the whole group of patients in both assessment sessions based on the highest Silhouette index. Clustered weightings of synergy structures did not significantly vary between sessions as indicated by a high mean dot product between homologous pre and

post clusters in the healthy limb (0.90 ± 0.03), confirming a general global consistency of the synergy structure over time (figure 3(C)). Paretic synergy clusters also presented a general high inter-session similarity in structure, with an inter-session mean scalar product of 0.88 ± 0.05 between paired clusters, respectively, with the cluster that involved the most distal extensor and flexor muscles (C1 in figure 3(D)) being the one with lower similarity index (i.e. with greater changes in synergy internal structure), as a consequence of a slightly increased co-activation of the biceps muscle. In comparison to functional healthy structures, paretic modular control exhibited a slight lower complexity characterized by a lower number of optimal clusters. This reduction in clusters dimension is derived from the merging of clusters C1 and C2 in the healthy limb (figure 3(C)) into a single cluster (C1) in the paretic limb (figure 3(D)), which indicates a general inability for selective fingers (ExtDig) or wrist (EXTCU) extensor activation. Moreover, the activity of these distal and most compromised muscles is accompanied by larger antagonist flexor (FLEX) and biceps (BIC) muscles activations (classical flexor synergy).

3.4. Pre-post therapy changes in muscle synergy features

We observed a significant general increase in $FSRI_{Global}$ (including all movements) as an effect of the intervention ($p = 0.015$), supporting a general increase in the correlation between the temporal

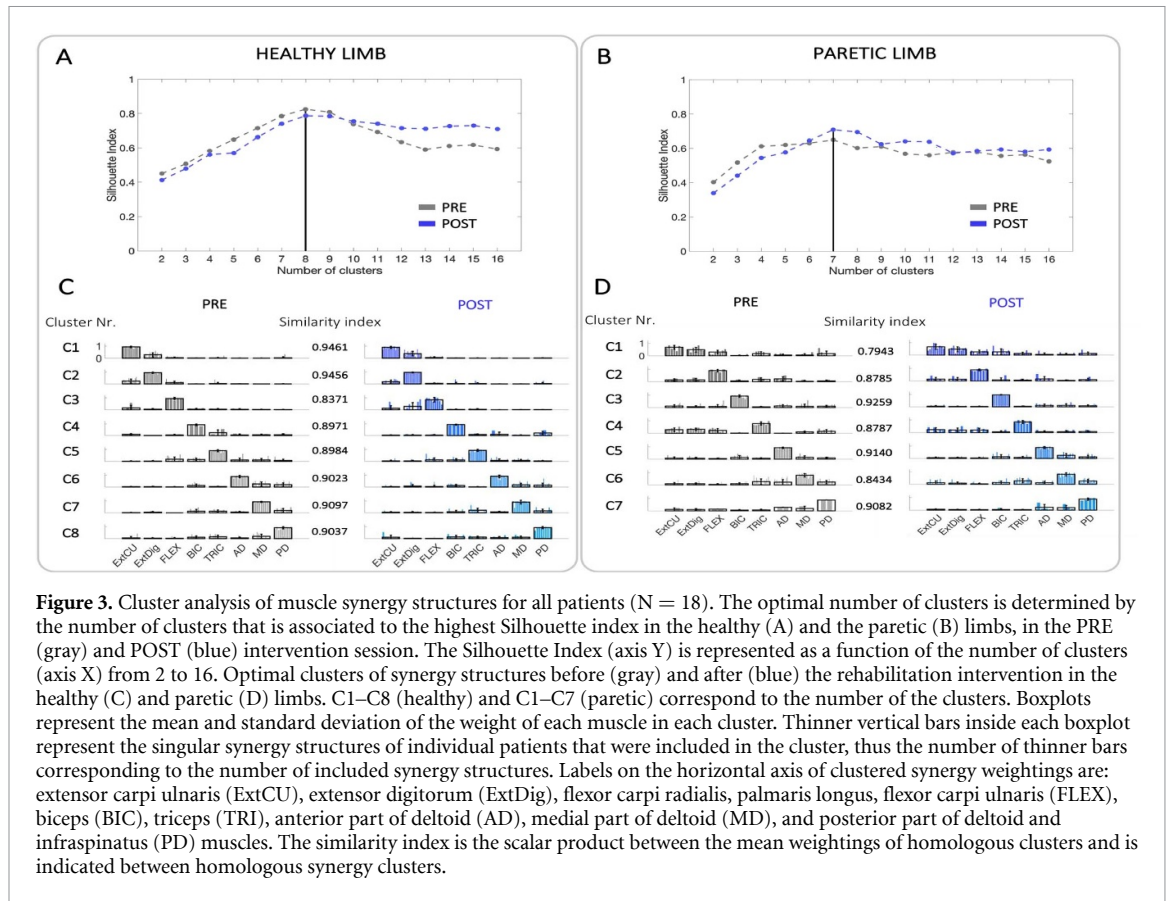


Figure 3. Cluster analysis of muscle synergy structures for all patients ($N = 18$). The optimal number of clusters is determined by the number of clusters that is associated to the highest Silhouette index in the healthy (A) and the paretic (B) limbs, in the PRE (gray) and POST (blue) intervention session. The Silhouette Index (axis Y) is represented as a function of the number of clusters (axis X) from 2 to 16. Optimal clusters of synergy structures before (gray) and after (blue) the rehabilitation intervention in the healthy (C) and paretic (D) limbs. C1–C8 (healthy) and C1–C7 (paretic) correspond to the number of the clusters. Boxplots represent the mean and standard deviation of the weight of each muscle in each cluster. Thinner vertical bars inside each boxplot represent the singular synergy structures of individual patients that were included in the cluster, thus the number of thinner bars corresponding to the number of included synergy structures. Labels on the horizontal axis of clustered synergy weightings are: extensor carpi ulnaris (ExtCU), extensor digitorum (ExtDig), flexor carpi radialis, palmaris longus, flexor carpi ulnaris (FLEX), biceps (BIC), triceps (TRI), anterior part of deltoid (AD), medial part of deltoid (MD), and posterior part of deltoid and infraspinatus (PD) muscles. The similarity index is the scalar product between the mean weightings of homologous clusters and is indicated between homologous synergy clusters.

recruitment of functional synergies by the healthy and paretic limbs after the intervention. In contrast, no significant differences were found in the optimal number of synergies in the paretic limb ($p = 0.85$), the inter-limb synergy structure preservation ($p = 0.123$), merging ($p = 0.058$) or the fractionation ($p = 0.797$) indexes between pre and post-therapy time points (figure 4).

3.5. Correlations between muscle synergy features and clinical scores

3.5.1. Number of synergies, preservation, merging and fractionation indexes

Before the intervention (pre), a weak but significant correlation was found between the number of optimal synergies found in the paretic side and aFMA ($r = 0.46891$, $p = 0.0496$) (figure S4(A)). The time elapsed since the trauma was also found to correlate proportionally with the merging index ($r = 0.48826$, $p = 0.0398$) (figure S4(B)) and negatively with the number of optimal paretic synergies ($r = -0.502$, $p = 0.0336$) (figure S4(C)).

Correlations between modifications in different synergy features and changes in clinical scores showed a weak but significant positive relationship between the change in the number of synergies and the general level of motor performance of the paretic limb (cFMA score) ($r = 0.486$, $p = 0.04$, figure S4(D)). Gains in aFMA score were also found to correlate with a reduction in the merging index ($r = -0.518$,

$p = 0.028$) (figure S4(E)), suggesting that an increase in the motor performance of the paretic limb could be attributed to a reduction in pathological co-activation of muscles. No other significant correlations were found between structural features and clinical scales values in pre or in their pre-post therapy differences (table 3).

3.5.2. FSRI

Pre-therapy level of motor function and the retained global ability to recruit healthy synergy modules (measured by FSRI_{Global}) showed a significant positive correlation between each other (figures 5(A)–(C)). In an additional analysis to investigate to what extent FSRI values evaluated during specific movements correlated with motor impairment, we observed that hFMA positively correlated with the FSRI of every individual movement, aFMA with FSRI during elbow extension (FSRI_{EE}) movement ($r = 0.5697$, $p = 0.0136$), and cFMA with FSRI_{SF} ($r = 0.5207$, $p = 0.0267$) and FSRI_{EE} ($r = 0.6787$, $p = 0.002$). As for the level of spasticity (MAS score), a significant negative correlation with FSRI was found exclusively for EE movement ($r = -0.48$, $p = 0.0431$). Note that, although not always significant, the sign of the correlation is generally positive for FMA scores and negative for MAS, what denotes a coherent relationship with motor performance in both cases (table 3).

Moreover, pre-post therapy changes in global FSRI (Δ FSRI) correlated significantly with changes

Table 3. Spearman's rank correlations coefficients (r) and significance (p -value) of values in pre (motor function) and pre-post therapy changes (motor recovery) in muscle synergy features with clinical scores.

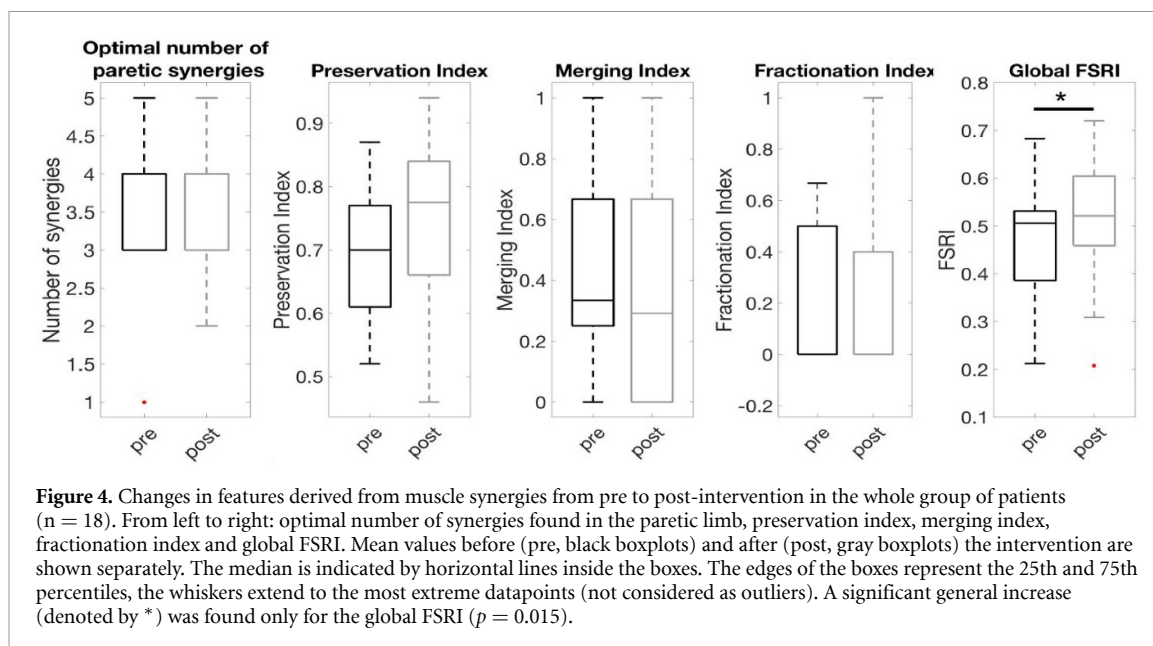
Clinical scores in PRE	Stats	Motor function										FSRI _{FE}	FSRI _{WE}	FSRI _{FE}
		Synergy structure features					FSRI							
		Num	P _{index}	M _{index}	F _{index}	F _{index}	FSRI _{SF}	FSRI _{SER}	FSRI _{EE}	FSRI _{WE}	FSRI _{FE}			
cFMA	r	0.342	-0.002	-0.007	0.193	0.668	0.521	0.410	0.679	0.250	0.465			
	p -value	0.164	0.993	0.979	0.443	0.0024^b	0.027^a	0.091	0.0020^b	0.317	0.052			
hFMA	r	-0.114	0.147	0.442	-0.177	0.670	0.8017	0.483	0.681	0.506	0.586			
	p -value	0.653	0.560	0.066	0.483	0.0023^b	0.0001^b	0.0425^a	0.0018^b	0.0320^a	0.0106^a			
aFMA	r	0.469	-0.085	-0.134	0.34	0.617	0.334	0.285	0.57	0.078	0.3169			
	p -value	0.0496^a	0.737	0.596	0.167	0.0063^b	0.175	0.252	0.0136^a	0.759	0.2000			
MAS	r	-0.195	0.184	0.184	0.15	-0.245	-0.201	-0.415	- 0.481	-0.036	-0.0818			
	p -value	0.438	0.464	0.466	0.55	0.326	0.424	0.087	0.0431^a	0.886	0.7470			
Chronicity	r	- 0.502	0.222	0.488	-0.09	0.365	0.336	0.0196	0.286	0.204	0.359			
	p -value	0.0336^a	0.375	0.0398^a	0.722	0.13634	0.173	0.938	0.249	0.417	0.144			

Δ Clinical scores	Stats	Motor recovery										Δ FSRI _{FE}	Δ FSRI _{WE}	Δ FSRI _{FE}
		Synergy structure features					FSRI							
		Δ Num	Δ P _{index}	Δ M _{index}	Δ F _{index}	Δ F _{index}	Δ FSRI _{SF}	Δ FSRI _{SER}	Δ FSRI _{EE}	Δ FSRI _{WE}	Δ FSRI _{FE}			
Δ cFMA	r	0.486	-0.362	-0.291	0.30	0.560	0.505	0.05	0.314	-0.040	0.357			
	p -value	0.04^a	0.140	0.240	0.226	0.0156^a	0.032^a	0.845	0.204	0.874	0.146			
Δ hFMA	r	0.22	-0.032	0.255	0.028	0.029	-0.151	-0.133	-0.164	-0.301	0.121			
	p -value	0.38	0.899	0.308	0.912	0.908	0.549	0.597	0.516	0.224	0.633			
Δ aFMA	r	0.452	-0.43	- 0.518	0.248	0.6974	0.716	0.100	0.453	0.082	0.372			
	p -value	0.06	0.075	0.028^a	0.322	0.0013^b	0.0008^b	0.691	0.059	0.747	0.128			
Δ MAS	r	0.375	-0.076	0.221	0.099	-0.0719	-0.255	-0.230	-0.149	0.19	0.174			
	p -value	0.125	0.764	0.378	0.697	0.777	0.307	0.358	0.555	0.451	0.490			

Statistically significant correlations are highlighted in bold.

^a $p < 0.05$.

^b $p < 0.01$.



in aFMA ($r = 0.6974$, $p = 0.0013$) and cFMA ($r = 0.5602$, $p = 0.0156$) but not hFMA ($r = 0.029$, $p = 0.908$), as shown in figures 5(D)–(F). Additionally, significant correlations were found between Δ cFMA and Δ FSRI_{SF} ($r = 0.505$, $p = 0.032$), as well as between Δ aFMA and Δ FSRI_{SF} ($r = 0.716$, $p = 0.0008$) (table 3). Generally, patients with a significant motor improvement after the intervention (i.e. increasing FMA scores) concurrently exhibited an increment in FSRI scores. Examples of the changes in FSRI value from PRE to POST of two representative patients with and without significant clinical improvement are shown in figure 6.

3.6. Effect of the BMI feedback contingency on muscle synergy features

When separated by feedback, the interaction between the intervention type and time was significant for FSRI variable during the finger extension (FE) movement only (FSRI_{FE}) (mixed ANOVA, $F_{1,16} = 5.59$, $p = 0.031$) (figure 7), which coincides with the motor task that was trained by all patients and most intensively in the BMI therapy. In fact, we observed that the experimental group increased their FSRI value during FE movement, whereas the control group who received random or contingent negative BMI feedback was characterized by a decrease in the correct temporal recruitment of functional synergies during this gesture. Post-hoc analyses revealed that the main effects for the TIME and FEEDBACK variables were not significant ($p > 0.05$). We also observed that the significance of the feedback type effect on the pre-post FSRI change presented values closer to significant p values for individual motor tasks that were trained with less intensity within the BMI intervention (elbow extension, $p = 0.12$) or movements that included BMI-trained tasks as sub-movements (shoulder flexion, including partial elbow extension

as sub-movement, $p = 0.158$), and furthest for movements that were not included in the undergone BMI interventions (shoulder external rotation, $p = 0.66$, and wrist extension, $p = 0.765$) (figure 7). Overall, mean FSRI values of individual movements were higher for the tasks involving most proximal joints (i.e. involving less impaired muscles) and lower for movements requiring most distal and therefore more compromised muscles (i.e. FSRI_{SF} was the highest, followed by FSRI_{SER}, FSRI_{EE}, FSRI_{WE} and finally FSRI_{FE}). The TIME \times FEEDBACK interaction was not found to be significant for the global FSRI either (mixed ANOVA, $F_{1,16} = 0.904$, $p = 0.356$). The task-specific FSRI values were generally higher for the control group before the intervention (PRE) in all movements except for SER (see figure 7). In fact, a similar tendency can be also observed in the clinical scores of motor function (cFMA, hFMA and aFMA) of the patients in PRE when divided in experimental (exp) and control feedback groups as shown in figure S5. This tendency is therefore in line with the significant correlations that we have found between the clinical scores of motor function (cFMA, hFMA and aFMA) and FSRI values (general and task-specific) in PRE.

4. Discussion

In this study we investigated diverse features derived from muscle synergies and evaluated their potential to reliably reflect the status and changes in neuromuscular control in a representative cohort of severely paralyzed stroke patients. Based on muscle synergy theory, we proposed a novel synergy-based muscle activity feature (FSRI) to measure the remaining ability of stroke patients to correctly recruit theoretically preserved functional muscle synergies based on their paretic muscle activity. Our analyses revealed that the degree of correlation of the temporal recruitment of a

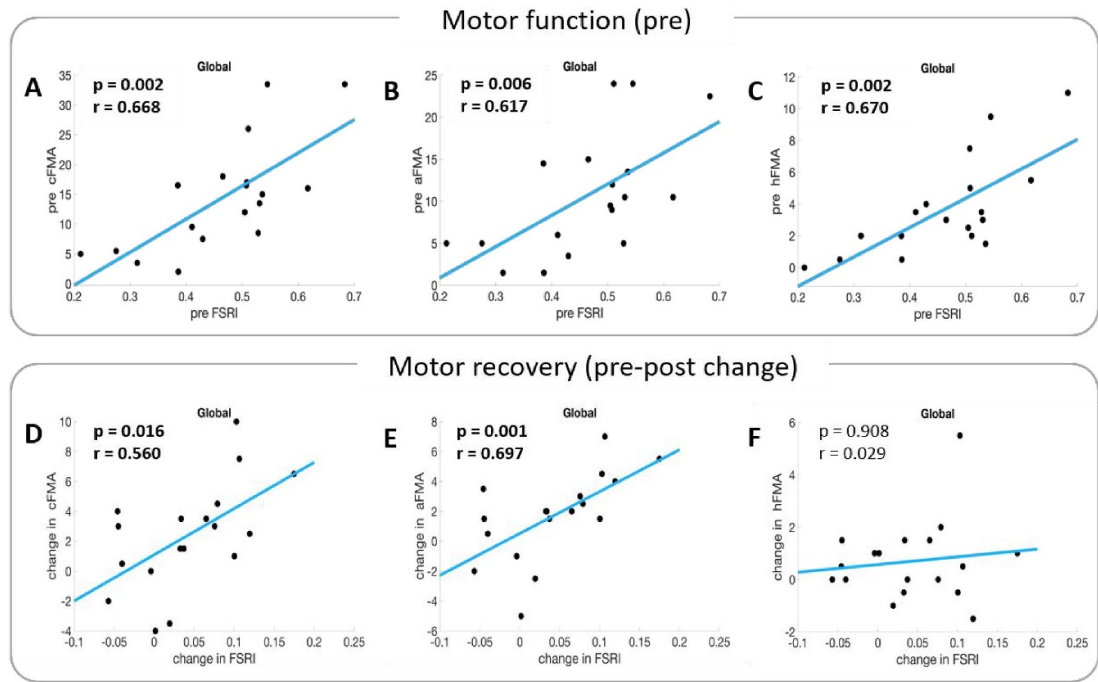


Figure 5. Correlations between FSRI and clinical scores. Above: Spearman's rank correlation coefficient (r) and its significance (p -value) between global FSRI and ordinal clinical scales (A) cFMA ($r = 0.668$, $p = 0.002$), (B) aFMA ($r = 0.617$, $p = 0.006$) and (C) hFMA ($r = 0.67$, $p = 0.0023$). Below: Spearman's rank correlation between the pre-post change in FSRI (Δ FSRI) and the change in ordinal clinical scales: (D) Δ cFMA ($r = 0.5602$, $p = 0.0156$), (E) Δ aFMA ($r = 0.6974$, $p = 0.0013$) and (F) Δ hFMA ($r = 0.029$, $p = 0.908$). Black dots show the FSRI value in pre (motor function, above) or pre-post change (motor recovery, below) (X axis) and clinical scores (Y axis) for each patient ($n = 18$) and the blue lines represent the regression lines. Significant correlations are highlighted in bold.

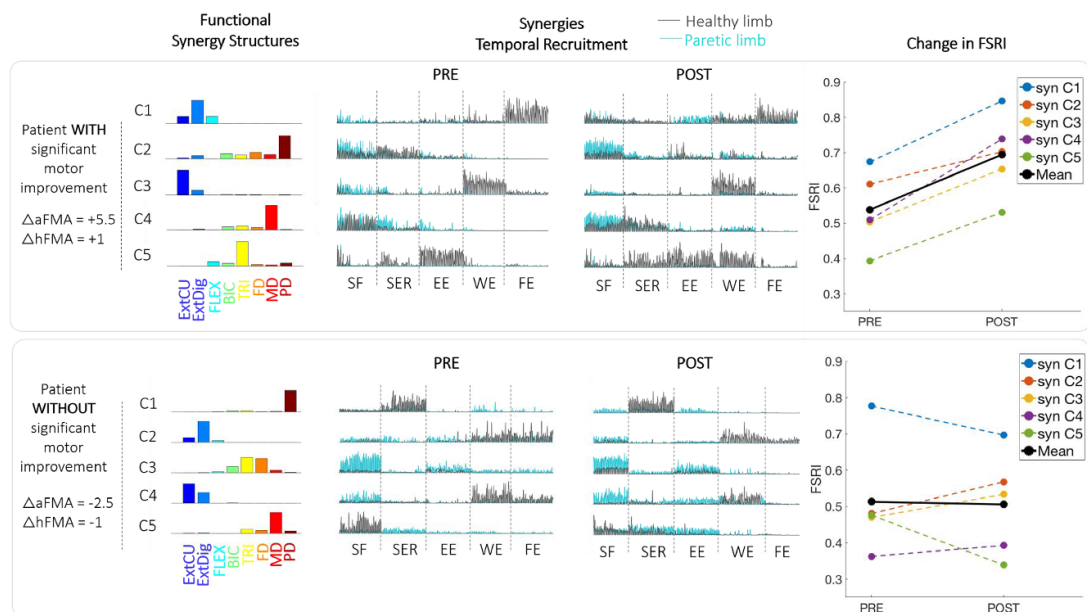
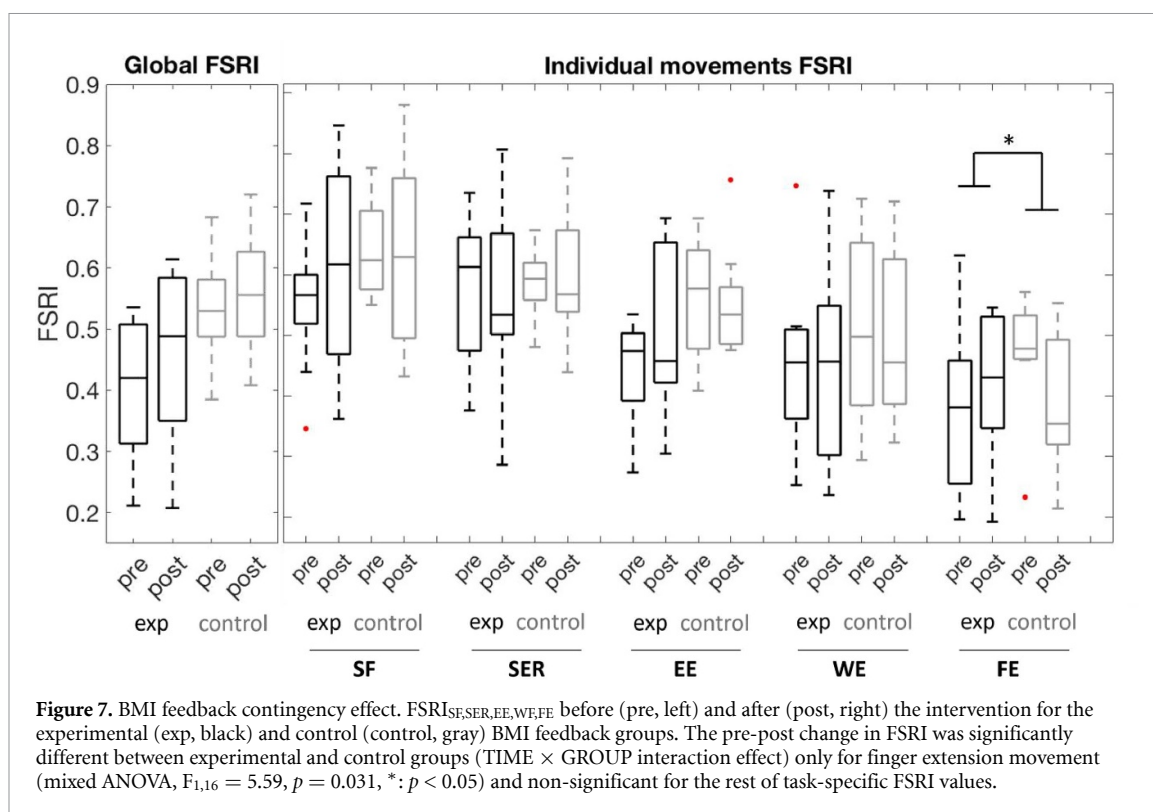


Figure 6. Changes in clinical scores and $FSRI_{Global}$ in two representative patients. Two representative patients with (above) and without (bottom) significant motor recovery denoted by positive and negative changes in FMA scores, respectively. Left: Set of functional synergy structures (C1)–(C5) extracted from the healthy limb muscles in measurement PRE. Middle: the respective temporal recruitment profiles calculated from healthy (gray) and paretic (blue) sEMG activity before (PRE) and after (POST) therapy. Trials of the temporal recruitment of each synergy during the five motor tasks (SF, SER, EE, WE, FE) were concatenated and normalized to the maximum amplitude the temporal activation of the synergy in the healthy limb for visualization. Right: changes in the global FSRI values from pre to post-intervention calculated from the temporal recruitment profiles (healthy and paretic) of each individual synergy structures (syn C1–syn C5, dashed lines) and the mean $FSRI_{Global}$ (black, continuous line).



set of functional muscle synergies between the paretic and healthy muscles could document motor performance more accurately than structure-based features at least for chronic patients with severe paresis. Moreover, a contingent positive proprioceptive feedback during BMI training was found to be relevant for the adaptation of the pathological temporal control of modular muscle control towards similar timings observed in the healthy patterns.

4.1. Reduced dimensionality and over-time consistency of synergy structures

On average, our data showed that less synergies would suffice for the same minimal EMG reconstruction criteria in the paretic limb in comparison to the healthy one (figure 3(A)) which is in line with previously reported results in severely affected chronic stroke patients [26, 52]. Cluster analysis revealed a global reduced dimensionality in paretic modular organization as indicated by a lower number of clusters in the paretic limb in comparison to the healthy side, commonly reported for stroke patients [52]. Additionally, we observed that both healthy and paretic muscle synergy clusters showed a high similarity in grouped synergy structures between the two different measurement times, indicating a consistent and repeatable modular organization of muscle control in the unaffected and affected ULs. Our results also evidence a lack of an independent control pattern of the extensor muscle of the fingers (since a similar cluster to healthy C2 with predominant fingers extensor activity is not present among the affected ones) in both measurements, which is precisely related to

the most compromised function in this cohort of patients that did not significantly recover hand function. Biceps activity was considerably more present in co-activation with wrist and fingers extensors in the paretic limb after the intervention (C1 in figure 3(D)), which could indicate that certain patients generated these ill-formed coupled activations that could be interpreted as maladaptive or compensatory mechanism. Furthermore, coactivation of deltoid muscles was also present in some patients, which is common in severely affected patients [44]. Generally, we found one or two primary muscles to have a high contribution in each healthy cluster structure, whereas mean weights of the rest of the muscles (secondary) were minimal, indicating an ability for isolated muscle recruitment. As for the paretic clusters, the contribution of the secondary muscles appeared to be higher (e.g. triceps, anterior deltoid and posterior deltoid in coactivation with main middle deltoid activity), denoting a larger muscle co-activation and lower muscle-specific recruitment, which has been previously reported ([23], supplementary material), indicating spasticity and/or maladaptive muscle co-activations typically found in chronic phases of stroke [53].

4.2. FSRI based on the theory of physically preserved muscle synergies after stroke

The generation of novel synergies or the recovery of missing healthy ones have been identified in combination with a motor recovery process [52]. However, according to the increasing evidence of altered temporal coefficients of muscle synergies

rather than their intrinsic structure [5, 28], the altered expression of paretic muscle synergies poststroke could also be understood as an implicit consequence of modified temporal activation of preserved synergies, rather than the creation of new synergetic structures or the modification of existing ones. In mildly affected patients with highly preserved synergy structures, an inter-limb comparison of synergy activations is feasible based on an identical set of structures extracted from pooled EMG activity of both limbs [23]. Nevertheless, on patients with higher impairment, temporal recruitment profiles are conventionally computed with respect to a set of paretic-healthy 'paired' or 'homologous' synergy weightings (of individual patients or group-averaged after clustering) exhibiting highest similarity [27, 28, 54]. These inter-limb comparisons must inevitably assume variabilities between the compared temporal recruitment profiles due to differences in the basis synergy structures, rather than in the neurophysiological conditions between limbs. Thus, and in contradiction to the increasing evidence that synergy structures might remain physically preserved in neuronal networks at brainstem and spinal levels [1, 8, 9], paretic temporal recruitment profiles are still commonly computed based on the pathologically expressed synergy structures extracted from paretic EMG rather than considering theoretically preserved functional modules. In our work, we alternatively considered a fixed and common set of synergy structures expressed in the healthy limb for the computation and subsequent comparison of temporal activation patterns between the limbs within each individual patient. We thereby considered these healthy synergies as a correct and functional model of synergy modules that could represent the potential motor units that the ipsilesional sensorimotor cortex should aim at correctly recruiting after a stroke in order to produce functional muscle activity. We also assumed that no pathological changes occur in synergy expression in the unaffected limb of a hemiplegic stroke patient with the elapse of time [5, 6, 55]. We therefore considered that the FSRI feature, a measurement of the temporal correlation between functional healthy synergy recruitment activation patterns expressed in the healthy and paretic EMG signals, can reflect the ability of supraspinal structures to recruit these functional muscle control modules. In fact, superior correlated activity of perilesional high-gamma activity and preserved synergy modules in comparison to abnormally expressed ones [56] supports the idea that cortical networks may still target at accessing remained functional control modules after stroke. Although FSRI values below maximum temporal correlation could be mainly ascribed to altered neuromuscular control, they could also be partially associated to different temporal activation strategies between right and left limbs previously demonstrated in healthy subjects [45].

4.3. FSRI as a reliable biomarker of motor function and recovery

Our results demonstrated a direct relationship between FSRI and motor function evidenced by significant correlations between FSRI_{Global} and UL clinical performance at all joint levels (arm, hand and combined FMA) before the intervention (figures 5(A)–(C)). In addition, although not always significant, the relationship between FSRI values and clinical scales showed a coherency with motor performance (i.e. positive correlation with FMA and negative with MAS scores). Moreover, changes in FSRI significantly correlated with longitudinal changes induced in aFMA and cFMA as an effect of the intervention, coinciding with the only clinical scores that presented a significant improvement in the overall group of patients (table 2, figure S2). Furthermore, higher values of task-specific FSRI for movements involving upper-arm proximal muscles (shoulder flexion) in contrast to lower FSRI during tasks involving most distal and affected muscles (fingers extension) suggested again the potential of this feature to describe the residual neuromuscular control of a patient. The results presented in this study suggest that the proposed FSRI feature could be potentially used as a reliable biomarker that represents the degree of preserved functional neural recruitment of muscle synergies during voluntary movement after stroke. However, it is important to note that muscle synergy calculation is potentially sensitive to intrinsic (biomechanical or task constraints) and extrinsic factors (selection and number of muscles used for factorization), which are not necessarily related to putative neural control [44]. Although the same group of muscles was used for every muscle synergy calculation to ensure comparability among subjects and measurements, it remains to be tested if the FSRI is a generally valid biomarker of motor function by evaluating this feature under different conditions independent of neural control (e.g. using different groups of muscles or during biomechanically constrained isometric motor tasks).

4.4. Poorer characterization of motor function and recovery by features based on inter-limb synergy structural differences

Different features based on muscle synergies have been proposed in the literature due to their potential to reflect underlying neurophysiological mechanisms of motor performance and modified control strategies in healthy subjects [45], as well as motor function and recovery in stroke [27]. The study of synergy dimensionality (optimal number of synergies) and synergy structures permits to quantify to what extent the modular organization of muscle control is still reflected in the paretic motor system of a patient after a stroke. Recent literature has mainly proposed three mechanisms to describe

the functional preservation and re-adaptation processes, either functional or maladaptive, that might occur at the post-injury central nervous system and can be captured in the peripheral system: preservation, merging and fractionation [23]. In our data, merged paretic synergies could be found in most of the patients (15/18), while fractionation mechanisms were less common (7/18), as previously reported in patients with severe paralysis [26]. Our correlation analysis between muscle synergy features and clinical scales before the intervention has served for the characterization of post-stroke motor function in a group of severely paralyzed chronic patients. In this cohort, the number of synergies extracted from the affected limb was found to weakly correlate with aFMA scores, suggesting an association between the number of synergies and the level of arm motor function as previously reported elsewhere for the upper [30] and lower limbs [48]. This analysis also revealed that the ratio of paretic modules that resulted from a merging process was proportional to the time elapsed after the stroke, suggesting that coactivation of muscle groups could be a result of maladaptive compensatory strategies adopted over time in response to the impairment caused by the lesion [57], which are more present in the chronic state than in the subacute phases [53]. Moreover, we found a higher number of muscle activity modules (i.e. more complex muscle coordination) in the paretic limb of patients with better arm performance (higher aFMA score) and more recent brain lesions (i.e. less time elapsed after the stroke). Furthermore, we found merging index negatively correlating with motor function, which is in line with previous work reported for lower limb motor function in subacute patients, where reduced merging levels correlated with increased motor performance measured in terms of muscle strength and gait kinematics [58]. In contrast to previous works on moderately-to-severely impaired stroke patients, this group of patients did not reveal any significant correlation between their merging index and motor impairment (i.e. FMA scores) [23, 26, 27], between their fractionation index and chronicity [23] or between the optimal number of paretic synergies and MAS scores [26]. Moreover, even in presence of significant upper arm recovery, we did not find substantial general changes in the weighting structures of muscle synergies as an effect of the intervention as previously reported elsewhere [28]. Thus, our results from the correlation between clinical scores and features derived from the inter-limb comparison of muscle synergy structures revealed that these features commonly used in literature do not always reliably describe the level and variations of motor performance, at least in severely paralyzed stroke patients. The fact that our results are not consistent with previous evidence might be partially ascribed to differences in the methods applied for the calculation of parameters and the patient cohort. Features derived from muscle

synergies have been defined and computed in slightly different manners in the literature, which has not allowed the field to unequivocally describe or standardize the alterations that occur in muscle coordination after a disruption at muscle synergy level. A standardized analysis of features based on muscles synergies would allow a better replicability of results in different cohorts of patients and a universal quantitative measurement of the underlying neural disruptions causing the impairment [59].

4.5. The relevance of proprioceptive BMI contingency on FSRI

Unlike movement therapy [30], robot-assisted therapy [28, 29, 49] or FES therapy [31, 32], to our knowledge, the effect of a BMI intervention in synergy expression had not been studied to date. In this first work analyzing the effects of the combination of BMI-controlled robot therapy and physiotherapy on muscle synergy enrolment in chronic stroke, we found a significant change in the temporal recruitment of synergies while structures remained consistent, similarly to previously reported effects of a robot-assisted therapy in acute patients [28]. The study on the relevance of the BMI feedback on task-specific FSRI revealed that the degree of correct temporal recruitment increased significantly greater in the experimental group in comparison to the control group exclusively for the finger extension assessment task, the gesture that was trained most intensively and by all patients under BMI operation. Although not significant, the level of the BMI feedback condition effect during therapy on movement-specific FSRI values coincided with the intensity of additionally trained motor tasks (i.e. elbow extension was trained only by some of the patients for a few sessions). Thus, our results indicate that training the modulation of sensorimotor brain oscillatory activity with a BMI does not necessarily affect the synergy modular expression but might facilitate a correct task-specific temporal modulation of synergies only when providing contingent positive proprioceptive feedback of motor-related neural correlates of specific motor tasks, even in chronic stroke. It is important to note that in our study, the experimental and control groups were not homogeneous with regard to their brain lesion location (subcortical or mixed), which has been demonstrated to influence the sensorimotor brain oscillatory activity modulation of stroke patients [60, 61]. Additionally, modifications in brain oscillatory activity have been recently associated with BMI control improvement and functional recovery undergoing this intervention in partly the same cohort of patients [62]. Therefore, changes in synergy recruitment could not be unequivocally ascribed to the BMI feedback type and they could be additionally conditioned by the lesion location. Unfortunately, our study does not explain how the observed modifications in muscle synergy temporal

recruitment were possibly originated by changes in descending cortical activity [45]. Protocols including concurrent brain and EMG activity recordings may allow to further verify the relationship between cortical activity and muscle synergy recruitment profiles as previously demonstrated for perilesional high-gamma oscillations and preserved synergy modules in a chronic stroke patient [56], as well as the existence of correlated adaptations in brain and muscle activity associated with recovery.

4.6. Clinical application of muscle synergies and FSRI

By no means conclusive due to the heterogeneity of the studied populations, various cross-sectional studies [5, 17, 22, 23, 26, 27, 44] have nonetheless permitted to a certain extent the characterization of the post-stroke muscle motor function based on muscle synergies [25]. However, although muscle synergies have been also proposed to characterize motor recovery [25], to date only a small number of studies have investigated over-time modifications in muscle synergies in groups of patients with a significant motor improvement in response to a rehabilitative intervention in longitudinal studies [28–32, 49]. Although clinical scales are considered the primary outcome measure in clinical trials, works investigating modifications in muscle synergies of patients undergoing a motor improvement process are essential to understand the neurophysiology of underlying mechanisms of motor recovery to design clinically effective therapies.

Several authors have proposed the idea of using features based on the reinforcement of muscle synergy recruitment in the paretic limb towards a healthy pattern [21, 36]. In this work, we designed a protocol to concurrently acquire the sEMG activity of paretic and healthy muscles of the UL during bilateral symmetric/mirrored attempted movements. This allowed us to measure the continuous temporal recruitment of non-pathological muscle activity from the non-paretic limb, which could serve as a healthy reference for continuous comparison with the paretic limb. The FSRI feature could therefore offer valuable patient-specific information about their global remaining capacity of correctly recruiting functional muscle synergies during bilateral intended motor tasks. More specifically, the individual study of each synergy activation profile (i.e. the individual nCC value of each synergy module) could help detect preserved or pathological patterns of recruitment of particular muscle ensembles, enabling the design of rehabilitative approaches to specifically reinforce or correct such patterns, respectively. A similar *mirroring* idea has been recently implemented as an interventional tool to prove continuous feedback of the similarity of paretic muscle activations to the healthy limb based on robotic exoskeleton kinematics decoding [63]. Thereby, mirror approaches allowing continuous

feedback of the similarity of paretic muscle activations to the healthy limb [63] could be applied to target features as the FSRI by providing specific real-time feedback of their pathological activations and retraining correct activation timing of functional muscle synergies [21, 35, 36] leveraging BMI or myoelectric interfaces [31, 64].

5. Conclusion

The FSRI feature can reflect the ability to recruit a healthy muscle modular control measured in the affected muscles and reliably document not only motor function but also motor recovery in stroke patients. We therefore propose that FSRI could be used as a potential biomarker for quantitative assessment of neuromuscular behavior to be targeted in approaches for motor rehabilitation.

Acknowledgments

We thank R Massimiliano, L Læer, O Yilmaz, F L Brasil, G Liberati, M R Curado, A Vyziotis, W Cho, M Agostini, E Soares, S Soekadar, A Caria and L G Cohen for their participation in data acquisition and experiment design.

Funding

This study was funded by the Fortune-Program of the University of Tübingen (2452-0-0/2), the Bundesministerium für Bildung und Forschung (AMORSA (FKZ-16SV7754), REHOME (V5GR2001M1007-01)), EUROSTARS (SubliminalHomeRehab (FKZ: 01QE2023C E! 113928)) and the Basque Government Science Program (SINIC-TUS (2018222036), MODULA (KK-2019/00018), Elkartek-EXOTEK (KK-2016/00083)). N Irastorza-Landa's work was funded by the Basque Government's scholarship for predoctoral students.


ORCID iDs

Nerea Irastorza-Landa  <https://orcid.org/0000-0003-3170-0459>

Eliana García-Cossio  <https://orcid.org/0000-0002-5490-9127>

Andrea Sarasola-Sanz  <https://orcid.org/0000-0001-6347-5431>

Niels Birbaumer  <https://orcid.org/0000-0002-6786-5127>

Ander Ramos-Murguialday  <https://orcid.org/0000-0002-1549-4029>

References

- [1] Bizzi E, Cheung V C K, d'Avella A, Saltiel P and Tresch M 2008 Combining modules for movement *Brain Res. Rev.* **57** 125–33

- [2] Ting L H and Macpherson J M 2005 A limited set of muscle synergies for force control during a postural task *J. Neurophysiol.* **93** 609–13
- [3] Tresch M C, Saltiel P, d'Avella A and Bizzi E 2002 Coordination and localization in spinal motor systems *Brain Res. Rev.* **40** 66–79
- [4] Saltiel P, Wyler-Duda K, d'Avella A, Tresch M C and Bizzi E 2001 Muscle synergies encoded within the spinal cord: evidence from focal intraspinal NMDA iontophoresis in the frog *J. Neurophysiol.* **85** 605–19
- [5] Cheung V C K, Piron L, Agostini M, Silvoni S, Turolla A and Bizzi E 2009 Stability of muscle synergies for voluntary actions after cortical stroke in humans *Proc. Natl. Acad. Sci.* **106** 19563–8
- [6] d'Avella A, Portone A, Fernandez L and Lacquaniti F 2006 Control of fast-reaching movements by muscle synergy combinations *J. Neurosci.* **26** 7791–810
- [7] Roh J, Cheung V C K and Bizzi E 2011 Modules in the brain stem and spinal cord underlying motor behaviors *J. Neurophysiol.* **106** 1363–78
- [8] McMorland A J C, Runnalls K D and Byblow W D 2015 A neuroanatomical framework for upper limb synergies after stroke *Front. Hum. Neurosci.* **9** 82
- [9] Overduin S A, d'Avella A, Carmena J M and Bizzi E 2012 Microstimulation activates a handful of muscle synergies *Neuron* **76** 1071–7
- [10] Bizzi E and Cheung V C K 2013 The neural origin of muscle synergies *Front. Comput. Neurosci.* **7** 1–6
- [11] d'Avella A and Lacquaniti F 2013 Control of reaching movements by muscle synergy combinations *Front. Comput. Neurosci.* **7** 1–7
- [12] d'Avella A, Saltiel P and Bizzi E 2003 Combinations of muscle synergies in the construction of a natural motor behavior *Nat. Neurosci.* **6** 300–8
- [13] Bernstein N 1967 *The Co-Ordination and Regulation of Movements* (Oxford: Pergamon Press) p 196 (available at: <https://books.google.es/books?id=mUhjzwEACAAJ>)
- [14] Diedrichsen J and Classen J 2012 Stimulating news about modular motor control *Neuron* **76** 1043–5
- [15] Ting L H, Chiel H J, Trumbower R D, Allen J L, McKay J L, Hackney M E and Kesar T M 2015 Neuromechanical principles underlying movement modularity and their implications for rehabilitation *Neuron* **86** 38–54
- [16] Cheung V C K 2007 Sensory modulation of muscle synergies for motor adaptation during natural behaviors (Cambridge: Massachusetts Institute of Technology) (<http://hdl.handle.net/1721.1/38519>)
- [17] Roh J, Rymer W Z, Perreault E J, Yoo S B and Beer R F 2013 Alterations in upper limb muscle synergy structure in chronic stroke survivors *J. Neurophysiol.* **109** 768–81
- [18] Dewald J P, Pope P S, Given J D, Buchanan T S and Rymer W Z 1995 Abnormal muscle coactivation patterns during isometric torque generation at the elbow and shoulder in hemiparetic subjects *Brain* **118** 495–510
- [19] Beer R F, Dewald J P A, Dawson M L and Rymer W Z 2004 Target-dependent differences between free and constrained arm movements in chronic hemiparesis *Exp. Brain Res.* **156** 458–70
- [20] Urrea O, Casals A and Jané R 2014 Synergy analysis as a tool to design and assess an effective stroke rehabilitation *Proc. Annual Int. Conf. IEEE Engineering in Medicine and Biology Society (Chicago, August 2014)* pp 3550–3
- [21] Cheung V C K, Niu C M, Li S, Xie Q and Lan N 2019 A novel FES strategy for poststroke rehabilitation based on the natural organization of neuromuscular control *IEEE Rev Biomed Eng.* **12** 154–67
- [22] Li S, Zhuang C, Niu C M, Bao Y, Xie Q and Lan N 2017 Evaluation of functional correlation of task-specific muscle synergies with motor performance in patients poststroke *Front. Neurol.* **8** 337
- [23] Cheung V C K, Turolla A, Agostini M, Silvoni S, Bennis C, Kasi P, Paganoni S, Bonato P and Bizzi E 2012 Muscle synergy patterns as physiological markers of motor cortical damage *Proc. Natl. Acad. Sci.* **109** 14652–6
- [24] Coscia M, Tropea P, Monaco V and Micera S 2018 Muscle synergies approach and perspective on application to robot-assisted rehabilitation *Rehabilitation Robotics* (San Diego, CA: Academic Press) pp 319–31
- [25] Casadio M, Tamagnone I, Summa S and Sanguineti V 2013 Neuromotor recovery from stroke: computational models at central, functional, and muscle synergy level *Front. Comput. Neurosci.* **7** 97
- [26] García-Cossio E, Broetz D, Birbaumer N and Ramos-Murguialday A 2014 Cortex integrity relevance in muscle synergies in severe chronic stroke *Front. Hum. Neurosci.* **8** 744
- [27] Pan B, Sun Y, Xie B, Huang Z, Wu J, Hou J, Liu Y, Huang Z and Zhang Z 2018 Alterations of muscle synergies during voluntary arm reaching movement in subacute stroke survivors at different levels of impairment *Front. Comput. Neurosci.* **12** 69
- [28] Tropea P, Monaco V, Coscia M, Posteraro F and Micera S 2013 Effects of early and intensive neuro-rehabilitative treatment on muscle synergies in acute post-stroke patients: a pilot study *J. Neuroeng. Rehabil.* **10** 103
- [29] Belfatto A, Scano A, Chiavenna A, Mastropietro A, Mrakic-Sposta S, Pittaccio S, Molinari Tosatti L, Molteni F and Rizzo G 2018 A multiparameter approach to evaluate post-stroke patients: an application on robotic rehabilitation *Appl. Sci.* **8** 2248
- [30] Hesam-Shariati N, Trinh T, Thompson-Butel A G, Shiner C T and McNulty P A 2017 A longitudinal electromyography study of complex movements in poststroke therapy. 2: changes in coordinated muscle activation *Front. Neurol.* **8** 277
- [31] Niu C M, Bao Y, Zhuang C, Li S, Wang T, Cui L, Xie Q and Lan N 2019 Synergy-based FES for post-stroke rehabilitation of upper-limb motor functions *IEEE Trans. Neural Syst. Rehabil. Eng.* **27** 256–64
- [32] Niu C M, Zhuang C, Bao Y, Li S, Lan N and Xie Q 2017 Synergy-based NMES intervention accelerated rehabilitation of post-stroke hemiparesis *Annual Meeting of the Association of Academic Physiatrists (Las Vegas, Nevada, USA)*
- [33] Trumbower R D, Ravichandran V J, Krutky M A and Perreault E J 2010 Contributions of altered stretch reflex coordination to arm impairments following stroke *J. Neurophysiol.* **104** 3612–24
- [34] Yakovenko S, Krouchev N and Drew T 2011 Sequential activation of motor cortical neurons contributes to intralimb coordination during reaching in the cat by modulating muscle synergies *J. Neurophysiol.* **105** 388–409
- [35] Yang N et al 2019 Temporal features of muscle synergies in sit-to-stand motion reflect the motor impairment of post-stroke patients *IEEE Trans. Neural Syst. Rehabil. Eng.* **27** 2118–27
- [36] Israely S, Leisman G, Machluf C C and Carmeli E 2018 Muscle synergies control during hand-reaching tasks in multiple directions post-stroke *Front. Comput. Neurosci.* **12** 10
- [37] Ramos-Murguialday A et al 2013 Brain-machine interface in chronic stroke rehabilitation: a controlled study *Ann. Neurol.* **74** 100–8
- [38] Crow J L and Harmeling-van der Wel B C 2008 Hierarchical properties of the motor function sections of the Fugl-Meyer assessment scale for people after stroke: a retrospective study *Phys. Ther.* **88** 1554–67
- [39] Curado M R et al 2015 Residual upper arm motor function primes innervation of paretic forearm muscles in chronic stroke after brain-machine interface (BMI) training *PLoS One* **10** e0140161
- [40] Ramos-Murguialday A et al 2019 Brain-machine interface in chronic stroke: randomized trial long-term follow-up *Neurorehabil. Neural Repair* **33** 188–98
- [41] Lee D D and Seung H S 1999 Learning the parts of objects by non-negative matrix factorization *Nature* **401** 788–91

- [42] Lee D D and Seung H S 2001 Algorithms for non-negative matrix factorization *Adv. Neural Inf. Process. Syst.* 556–62
- [43] Tresch M C, Cheung V C K and d'Avella A 2006 Matrix factorization algorithms for the identification of muscle synergies: evaluation on simulated and experimental data sets *J. Neurophysiol.* **95** 2199–212
- [44] Roh J, Rymer W Z and Beer R F 2015 Evidence for altered upper extremity muscle synergies in chronic stroke survivors with mild and moderate impairment *Front. Hum. Neurosci.* **9** 6
- [45] Pellegrino L, Coscia M and Casadio M 2020 Muscle activities in similar arms performing identical tasks reveal the neural basis of muscle synergies *Exp. Brain Res.* **238** 121–38
- [46] Torricelli D, Barroso F, Coscia M, Alessandro C, Lunardini F, Bravo Esteban E and d'Avella A 2016 Muscle synergies in clinical practice: theoretical and practical implications *Emerging Therapies in Neurorehabilitation II Biosystems (Biosystems & Biorobotics vol 10)* ed Pons J L, Raya R and González J (Berlin: Springer) 251–72
- [47] Cheung V C K, d'Avella A, Tresch M C and Bizzi E 2005 Central and sensory contributions to the activation and organization of muscle synergies during natural motor behaviors *J. Neurosci.* **25** 6419–34
- [48] Clark D J, Ting L H, Zajac F E, Neptune R R and Kautz S A 2010 Merging of healthy motor modules predicts reduced locomotor performance and muscle coordination complexity post-stroke *J. Neurophysiol.* **103** 844–57
- [49] Pierella C et al 2020 A multimodal approach to capture post-stroke temporal dynamics of recovery *J. Neural Eng.* **17** 045002
- [50] Coscia M et al 2014 The effect of arm weight support on upper limb muscle synergies during reaching movements *J. NeuroEngineering Rehabil.* **11** 22
- [51] Pale U, Atzori M, Müller H and Scano A 2020 Variability of muscle synergies in hand grasps: analysis of intra- and inter-session data *Sensors* **20** 4297
- [52] Coscia M et al 2019 Training muscle synergies to relearn movement: current perspectives and future trends *Converging Clinical and Engineering Research on Neurorehabilitation III vol 21* (Berlin: Springer) pp 226–30
- [53] Gizzi L, Nielsen J F, Felici F, Ivanenko Y P and Farina D 2011 Impulses of activation but not motor modules are preserved in the locomotion of subacute stroke patients *J. Neurophysiol.* **106** 202–10
- [54] Scano A, Chiavenna A, Malosio M, Molinari Tosatti L and Molteni F 2017 Muscle synergies-based characterization and clustering of poststroke patients in reaching movements *Front. Bioeng. Biotechnol.* **5** 62
- [55] D'Avella A, Fernandez L, Portone A and Lacquaniti F 2008 Modulation of phasic and tonic muscle synergies with reaching direction and speed *J. Neurophysiol.* **100** 1433–54
- [56] Godlove J, Gulati T, Dichter B, Chang E and Ganguly K 2016 Muscle synergies after stroke are correlated with perilesional high gamma *Ann. Clin. Transl. Neurol.* **3** 956–61
- [57] Raghavan P, Santello M, Gordon A M and Krakauer J W 2010 Compensatory motor control after stroke: an alternative joint strategy for object-dependent shaping of hand posture *J. Neurophysiol.* **103** 3034–43
- [58] Hashiguchi Y et al 2016 Merging and fractionation of muscle synergy indicate the recovery process in patients with hemiplegia : the first study of patients after subacute stroke *Neural Plast.* **2016** 5282957
- [59] Safavynia S A, Torres-Oviedo G and Ting L H 2011 Muscle synergies: implication for clinical evaluation and rehabilitation of movement *Top Spinal Cord Inj Rehabil.* **17** 16–24
- [60] López-Larraz E, Ray A M, Birbaumer N and Ramos-Murguialday A 2019 Sensorimotor rhythm modulation depends on resting-state oscillations and cortex integrity in severely paralyzed stroke patients *9th Int IEEE/EMBS Conf Neural Eng NER 2019 9th Int. IEEE/EMBS Conf. on Neural Engineering (NER) (San Francisco, USA) (IEEE)* pp 37–40
- [61] Ray A M, López-Larraz E, Figueiredo T C, Birbaumer N and Ramos-Murguialday A 2017 Movement-related brain oscillations vary with lesion location in severely paralyzed chronic stroke patients *39th Annual Int. Conf. of the IEEE Engineering in Medicine and Biology Society (EMBC)* pp 1664–7
- [62] Ray A M, Figueiredo T D C, López-Larraz E, Birbaumer N and Ramos-Murguialday A 2020 Brain oscillatory activity as a biomarker of motor recovery in chronic stroke *Hum. Brain Mapp.* **41** 1296–308
- [63] Sarasola-Sanz A, Irastorza-Landa N, López-Larraz E, Shiman F, Spüler M, Birbaumer N and Ramos-Murguialday A 2018 Design and effectiveness evaluation of mirror myoelectric interfaces: a novel method to restore movement in hemiplegic patients *Sci. Rep.* **8** 16688
- [64] Lunardini F, Casellato C, d'Avella A, Sanger T D and Pedrocchi A 2016 Robustness and reliability of synergy-based myocontrol of a multiple degree of freedom robotic arm *IEEE Trans. Neural Syst. Rehabil. Eng.* **24** 940–50